Expanded View Figures

Figure EV1. Depletion of gut microbiota leads to relatively minor changes in the blood vasculature of intestinal villi.

A Images and comparisons of $CD31^+$ blood vessel (BV) densities and VEGFR2 expression (presented as relative fluorescent intensity (FI)) in the tip portion of villi in the jejunum of vehicle- or ABX-treated mice. Scale bars, 100 μm. AU, arbitrary unit. Each dot indicates mean value of 5–10 villi (n = 6 mice/group).

B Representative images of button-like, discontinuous VE-cadherin junction in the lymphatic capillary of ear skin (left) and zipper-like, continuous VE-cadherin junction in the collecting lymphatic vessel of mesentery (right). Note that LECs in lymphatic capillary are $Prox1^+$ $LYVE\text{-}1^+$, while LECs in lymphatic collector are $Prox1^+$ $LYVE\text{-}1^-$. Scale bars, 50 μm.

C Images of VE-cadherin LEC junctions in $CD31^+/LYVE\text{-}1^-$ blood capillary plexus of jejunum between vehicle- and ABX-treated mice. Note no difference in blood endothelial cell junctions of capillary plexus in villi between vehicle- and ABX-treated mice. Scale bars, 100 μm.

Data information: Data are represented as means ± SD. $^{**}P < 0.01$ versus vehicle-treated mice by two-tailed unpaired Student's t-test.

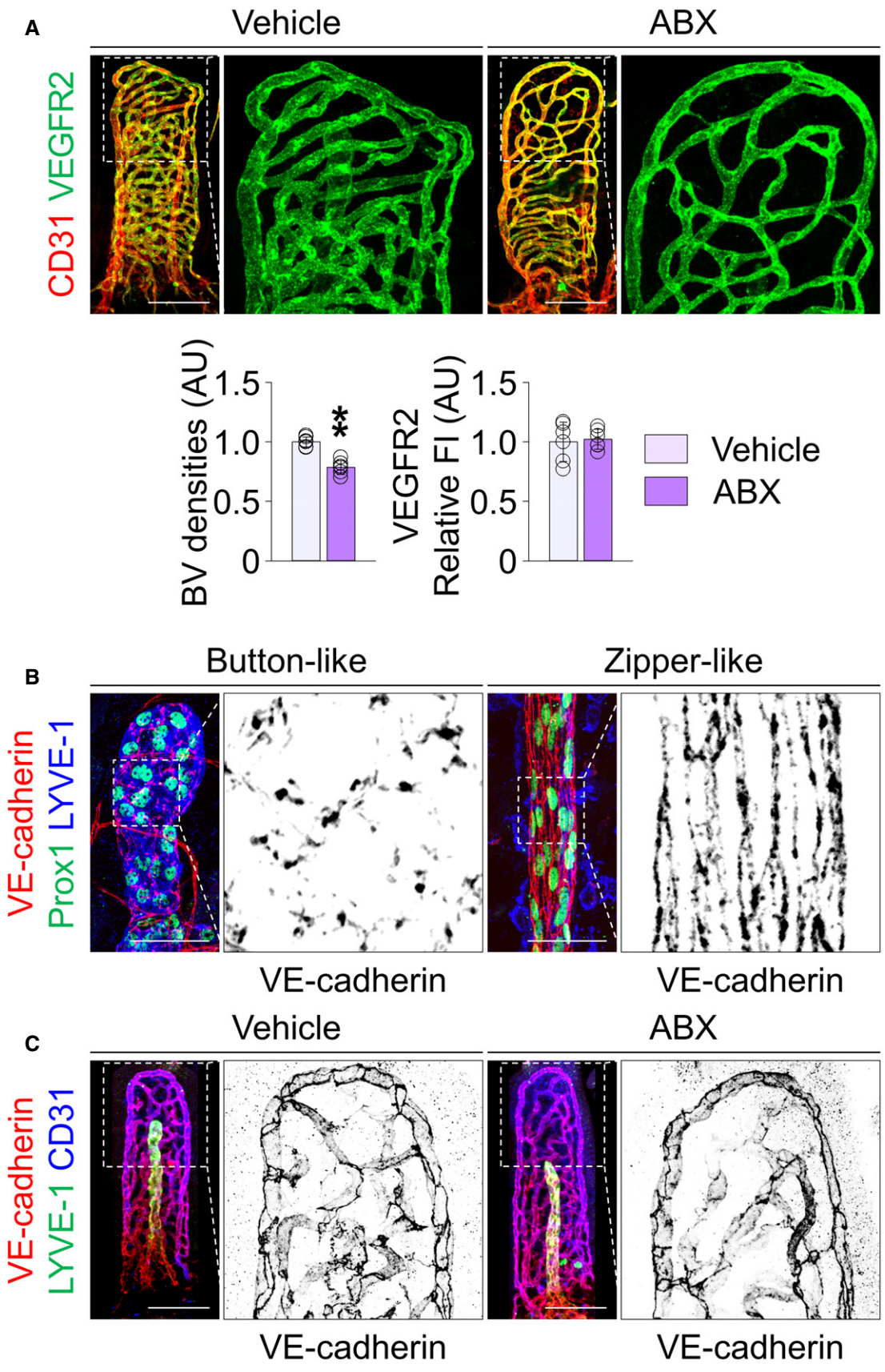

Figure EV1.

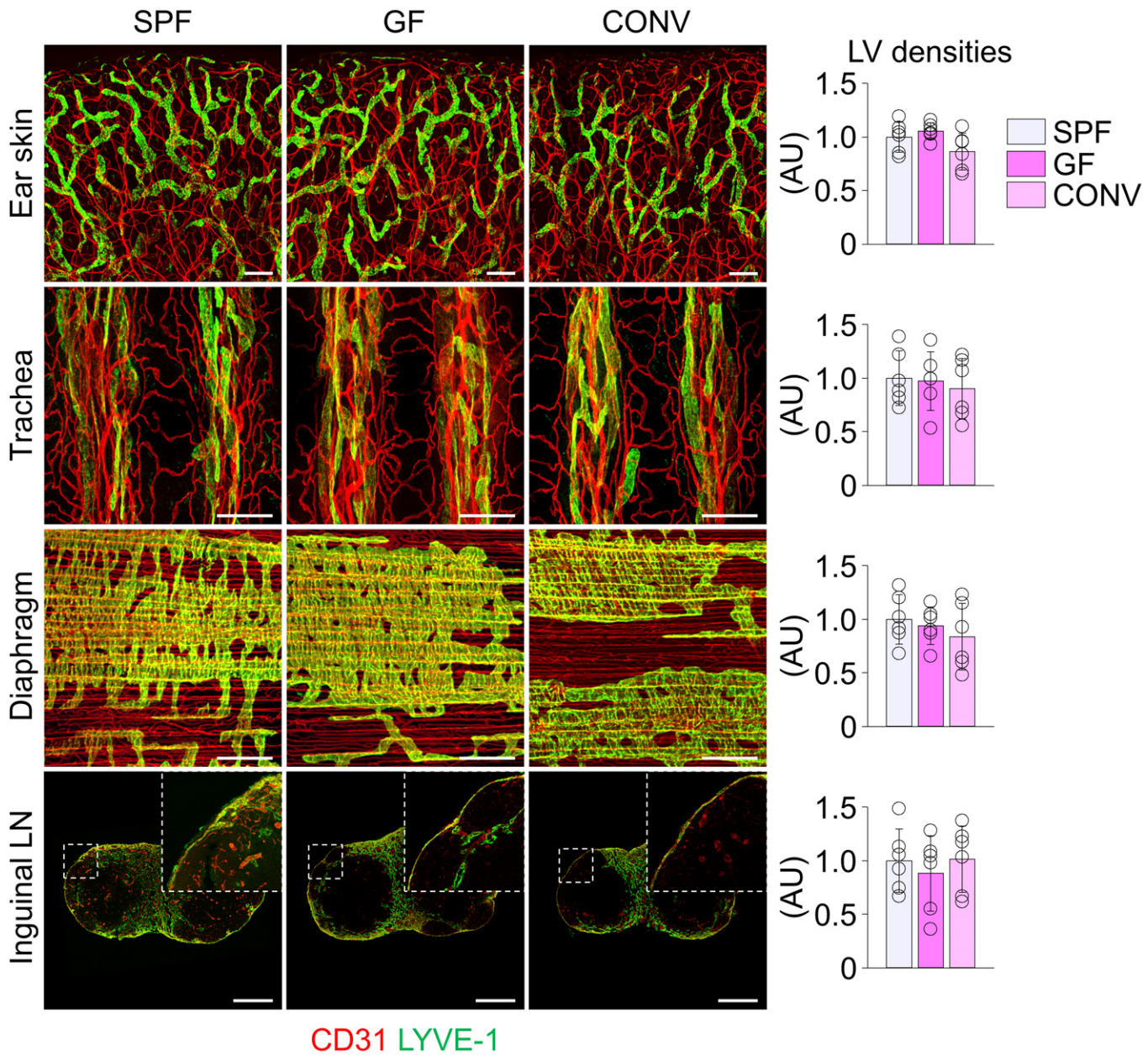

Figure EV2. The role of microbiota in the development of extra-intestinal lymphatics is dispensable.

Images and comparisons of LYVE-1$^+$ lymphatic vessel (LV) densities in the ear skin, trachea, diaphragm, and inguinal LN from SPF, GF, and CONV mice. AU, arbitrary unit. All scale bars, 200 μm. Each dot indicates mean value of five sites in a mouse (n = 6 mice/group). Data are represented as means ± SD.

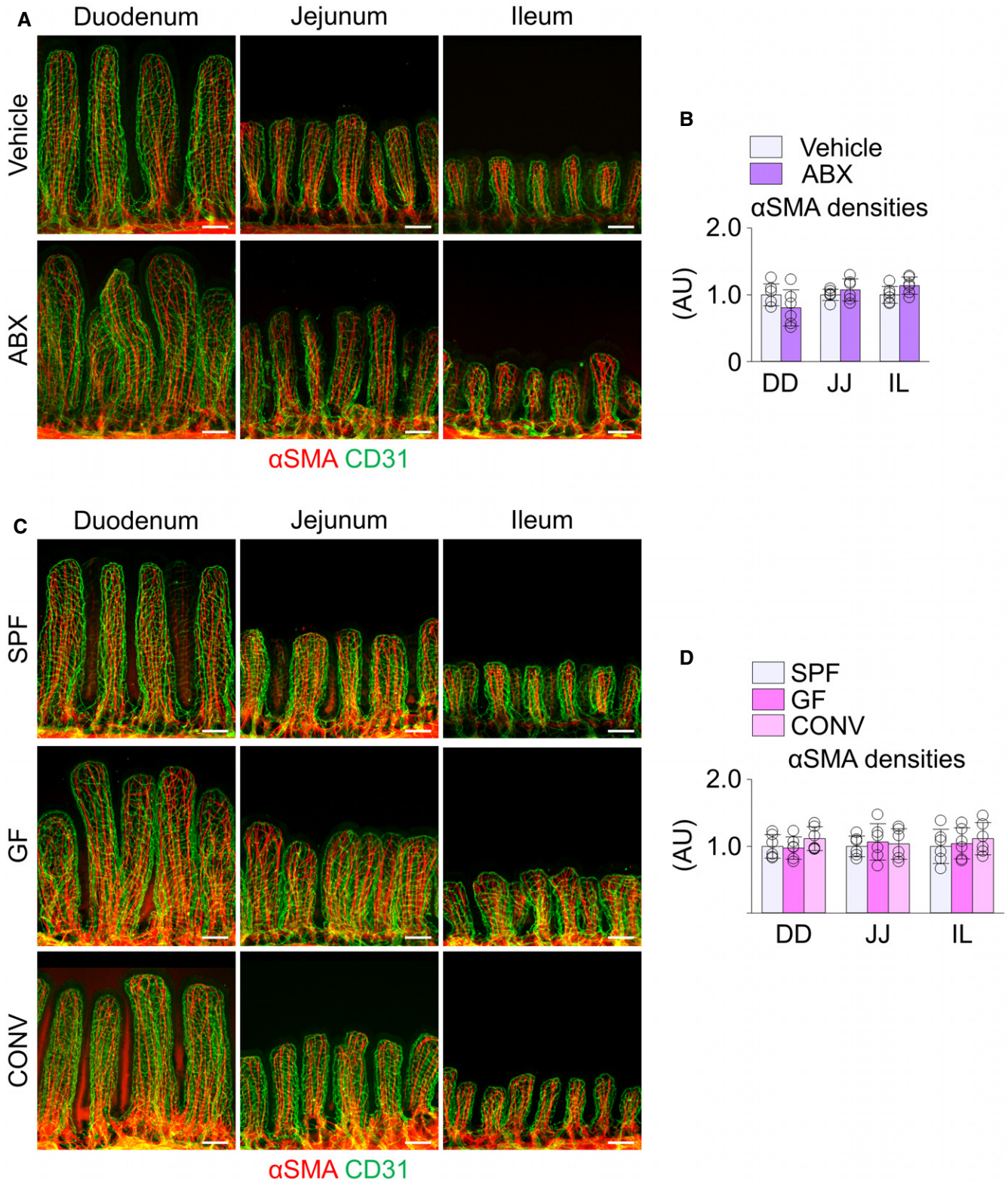

Figure EV3. The density of SMCs in the villi is independent of gut microbiota.

A–D Images and comparison of αSMA$^+$ SMCs in the villi of duodenum (DD), jejunum (JJ), and ileum (IL) from vehicle- or ABX-treated mice (A and B) and from SPF, GF, and CONV mice (C and D). Each dot indicates mean value of five sites in a mouse (n = 6 mice/group). AU, arbitrary unit. Scale bars, 100 μm. Data are represented as means ± SD.

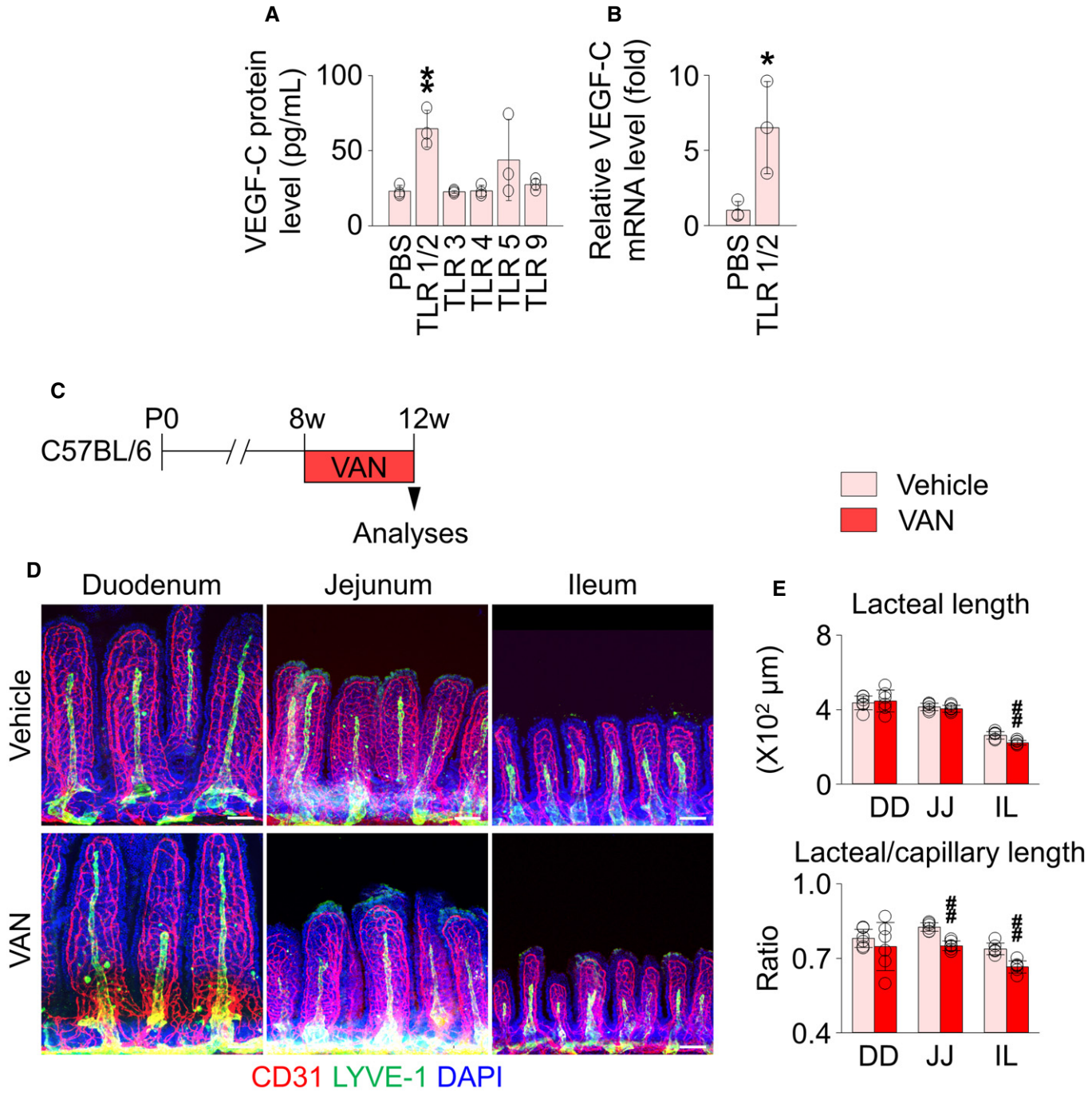

Figure EV4. The stimulation of a specific TLR subtype promotes the VEGF-C production in the intestinal macrophages.

A Measurement of VEGF-C protein level in the culture media after stimulation of primary intestinal macrophages with specific TLR agonists (n = 3). The following TLR agonists at indicated concentrations were treated: palmitoyl-3-cysteineserine-lysine-4 (TLR1/2 agonist, 1 μg/ml), poly(I-C) (TLR3 agonist, 10 μg/ml), lipopolysaccharide (TLR4 agonist, 5 μg/ml), flagellin (TLR5 agonist, 0.1 mg/ml), or bacterial DNA (TLR9 agonist, 10 μg/ml).

B Comparisons of mRNA levels of VEGF-C in intestinal macrophages with or without stimulation of TLR1/2 (n = 3). The relative levels are presented as fold (PBS as 1).

C Diagram for oral vancomycin (VAN) treatment in 8-week-old C57BL/6 mice.

D, E Images and comparisons of absolute and relative lacteal lengths in duodenum (DD), jejunum (JJ), and ileum (IL) of vehicle- and vancomycin-treated mice. Each dot indicates mean value of 5–10 villi in a mouse (n = 6 mice/group). All scale bars, 100 μm.

Data information: Data are represented as means ± SD. *P < 0.05, **P < 0.01 versus PBS by one-way ANOVA with Dunnett's multiple comparison test (A) and by two-tailed unpaired Student's t-test (B). ##P < 0.01 versus vehicle-treated mice by two-tailed unpaired Student's t-test (E).

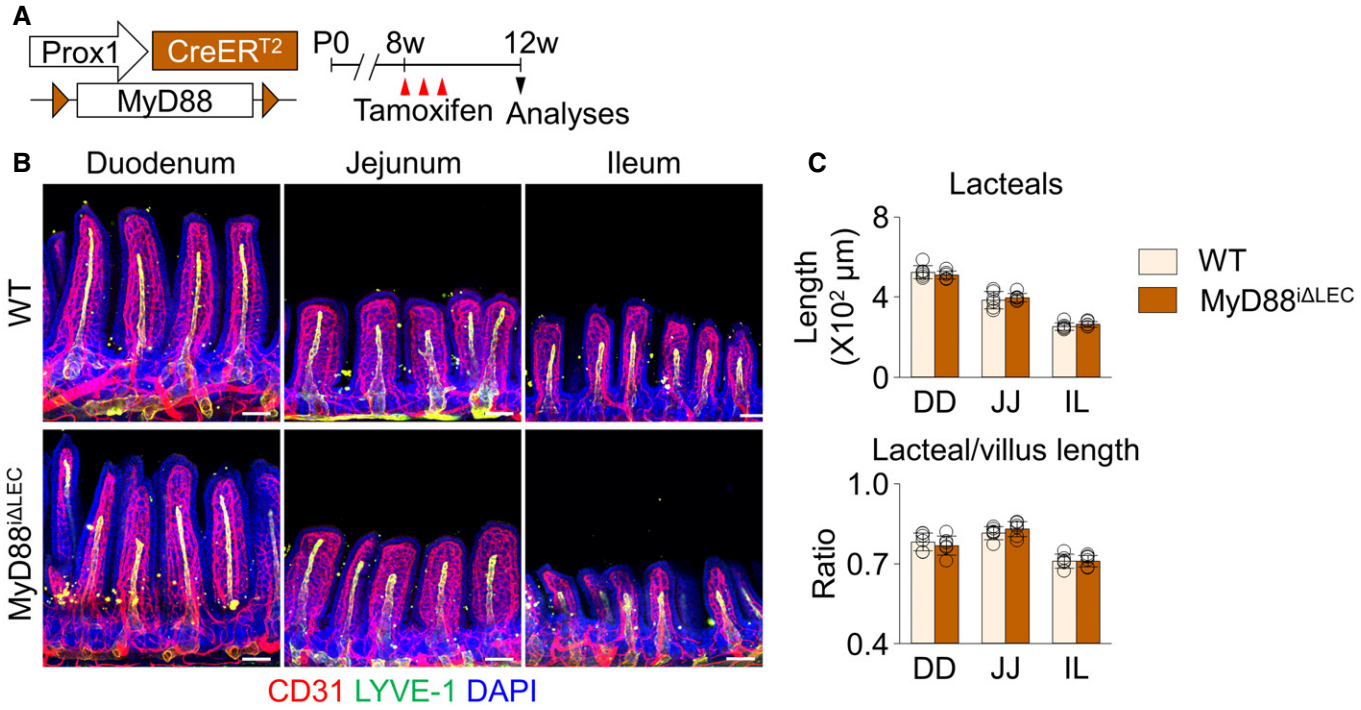

Figure EV5. LEC-specific ablation of MyD88 does not affect lacteal integrity.

A Diagram for LEC-specific ablation of MyD88 in adult mice (MyD88$^{i\Delta LEC}$). Tamoxifen was injected subcutaneously every other day for three times.

B, C Images and comparisons of absolute and relative lacteal lengths in duodenum (DD), jejunum (JJ), and ileum (IL) of wild-type (WT) and MyD88$^{i\Delta LEC}$ mice. All scale bars, 100 μm. Each dot indicates mean value of 5–10 villi in a mouse (n = 6 mice/group). Data are represented as means ± SD.